Langmuir
Article
pubs.acs.org/Langmuir

Novel Nanocomposites Made of Boron Nitride Nanotubes and a Physical Gel

Suman K. Samanta,[†] A. Gomathi,[‡] Santanu Bhattacharya,*[,†] and C. N. R. Rao*[,‡]

[†]*Department of Organic Chemistry, Indian Institute of Science, Bangalore, India, and* [‡]*Chemistry and Physics of Materials Unit and New Chemistry Unit, Jawaharlal Nehru Centre for Advanced Scientific Research, Bangalore, India*

Received March 23, 2010. Revised Manuscript Received May 10, 2010

This article describes successful incorporation of multiwalled boron nitride nanotubes (BNNTs) and various functionalized BNNTs by Lewis bases such as trioctylamine (TOA), tributylamine (TBA), and triphenylphosphine (TPP), etc., in organogels formed by triphenylenevinylene (TPV)-based low molecular weight gelator (LMWG) in toluene and consequent characterization of the resulting gel nanocomposites. Functionalized BNNTs were synthesized first, and the presence of tubular structures with high aspect ratio and increased diameter compared to the starting BNNTs was confirmed by SEM, TEM, and Raman spectroscopy. The micrographs of composites of **1** and BNNTs showed evidence of wrapping of the gelator molecules on to the BNNT surface presumably brought about by $\pi-\pi$ stacking and van der Waals interactions. This leads to the formation of densely packed and directionally aligned fibrous networks. Such "reinforced" aggregation of the gelator molecules in presence of doped BNNTs led to an increase in the sol-to-gel transition temperature and the solidification temperature of the gel nanocomposites as revealed from differential scanning calorimetry. Rheological investigations of the gel nanocomposites indicate that the flow properties of the resulting materials become resistant to applied stress upon incorporation of even a very low wt % of BNNTs. Finally, the increase in thermal conductivity of the nanocomposite compared to the gelator alone was observed for the temperature range of 0−60 °C which may make these composites potentially useful in various applications depending on the choice and the amount of BNNT loading in the composite.

Introduction

Boron nitride nanotubes (BNNTs) have attracted widespread attention due to their high aspect ratio,[1a] extraordinary mechanical properties,[1b,c] electrical insulating ability,[1d,e] high thermal conductivity,[1f−h] robustness to oxidation,[1i] and optical emitting properties.[1j,k] Because of their isoelectronic character and structural similarity, BNNTs and carbon nanotubes (CNTs) have certain properties which are comparable.[2] In several respects, however, BNNTs possess many advantageous properties compared to those of CNTs. For example, BNNTs are wide-band-gap semiconductors (5.2−5.8 eV) independent of diameter and chirality,[3a−d] and the nanoscale semiconducting properties can be operated in hazardous oxidative environments at high temperatures.[3e] Compared with CNTs, BNNTs also possess higher chemical stability and are transparent to visible light.[4] Polymer-based nanocomposites containing BNNTs offer wide range applications in optoelectronics, light-harvesting, and related phenomena.[5] In addition, BNNTs manifest improved thermal properties[6a] and were used as insulating composites of high thermal conductivity[6b] as in BNNTs; the thermal transfer mainly takes place via the phonons, not electrons.[6c]

Since solubilization of BNNTs is an important prerequisite to make BNNT useful, considerable effort has been devoted toward their solubilization via functionalization and wrapping with molecules such as quinuclidine,[7a] amine and phosphine,[7b] DNA,[7c] protein,[7d] polyaromatic systems, e.g., perylenes (PTAS)[7e] and phthalocyanines,[5] and various polymers such as poly(ethylene glycol),[7f] polyanilines (PANI),[4] polystyrene,[6a] and polyphenylene−vinylenes (PmPV).[7g] Covalent functionalization by amidation was also attempted to achieve their facial solubilization.[1e,4] However, the covalent functionalization induces defects in the nanotubes leading to the shortening of their aspect ratio, affecting the structure and electronic properties.[4] Therefore, nanocomposites are best developed through noncovalent functionalization.

*Corresponding authors: Fax 91-80-23600529, Tel 91-80-22932664, e-mail sb@orgchem.iisc.ernet.in (S.B.); Fax +91-80-8462760, Tel 91-80-23653075, e-mail cnrrao@jncasr.ac.in (C.N.R.).

(1) (a) Chen, H.; Chen, V.; Liu, Y.; Fu, L.; Huang, C.; Llewellyn, D. *Chem. Phys. Lett*. **2008**, *463*, 130. (b) Chopra, N. G.; Zettl, A. *Solid State Commun*. **1998**, *105*, 297. (c) Bettinger, H. F.; Dumitrica, T.; Scuseria, G. E.; Yakobson, B. I. *Phys. Rev. B: Condens. Matter* **2002**, *65*, 41406. (d) Zhi, C. Y.; Bando, Y.; Tang, C. C.; Huang, Q.; Golberg, D. *J. Mater. Chem*. **2008**, *18*, 3900. (e) Blase, X.; Rubio, A.; Louie, S. G.; Cohen, M. L. *Europhys. Lett*. **1994**, *28*, 335. (f) Han, W. Q.; Mickelson, W.; Cumings, J.; Zettl, A. *Appl. Phys. Lett*. **2002**, *81*, 1110. (g) Xiao, Y.; Yan, X. H.; Xiang, J.; Mao, Y. L.; Zhang, Y.; Cao, J. X.; Ding, J. W. *Appl. Phys. Lett*. **2004**, *84*, 4626. (h) Xiao, Y.; Yan, X. H.; Cao, J. X.; Ding, J. W.; Mao, Y. L.; Xiang, J. *Phys. Rev. B* **2004**, *69*, 205415. (i) Xiao, Y.; Yan, X. H.; Xiang, J.; Mao, Y. L.; Zhang, Y.; Cao, J. X.; Ding, J. W. *Appl. Phys. Lett*. **2004**, *84*, 4626. (j) Lauret, J. S.; Arenal, R.; Ducastelle, F.; Loiseau, A. *Phys. Rev. Lett*. **2005**, *94*, 037405. (k) Jaffrennou, P.; Donatini, F.; Barjon, J.; Lauret, J. S.; Maguer, A.; Attal-Tretout, B.; Ducastelle, F.; Loiseau, A. *Chem. Phys. Lett*. **2007**, *442*, 372.

(2) Golberg, D.; Bando, Y.; Tang, C.; Zhi, C. *Adv. Mater*. **2007**, *19*, 2413.

(3) (a) Rubio, A.; Corkill, J. L.; Cohen, M. L. *Phys. Rev. B: Condens. Matter* **1994**, *49*, 5081. (b) Radosavljevi, M.; Appenzeller, J.; Derycke, V.; Martel, R.; Avouris, Ph.; Loiseau, A.; Cochon, J.-L.; Pigache, D. *Appl. Phys. Lett*. **2003**, *82*, 4131. (c) Cumings, J.; Zettl, A. *Solid State Commun*. **2004**, *129*, 661. (d) Ishigami, M.; Sau, J. D.; Aloni, S.; Cohen, M. L.; Zettl, A. *Phys. Rev. Lett*. **2005**, *94*, 56804. (e) Tang, C. C.; Bando, Y. *Appl. Phys. Lett*. **2003**, *83*, 659.

(4) Zhi, C.; Bando, Y.; Tang, C.; Honda, S.; Sato, K.; Kuwahara, H.; Golberg, D. *Angew. Chem., Int. Ed*. **2005**, *44*, 7932.

(5) Huang, Q.; Sandanayaka, A. S. D.; Bando, Y.; Zhi, C.; Ma, R.; Shen, G.; Golberg, D.; Zhao, J.; Araki, Y.; Ito, O.; Gao, L. *Adv. Mater*. **2007**, *19*, 934.

(6) (a) Zhi, C.; Bando, Y.; Terao, T.; Tang, C.; Kuwahara, H.; Golberg, D. *Adv. Funct. Mater*. **2009**, *19*, 1857. (b) Jacoby, M. *Chem. Eng. News* **2004**, *82*, 35–34. (c) Chang, C. W.; Fennimore, A. M.; Afanasiev, A.; Okawa, D.; Ikuno, T.; Garcia, H.; Li, D.; Majumdar, A.; Zettl, A. *Phys. Rev. Lett*. **2006**, *97*, 085901.

(7) (a) Maguer, A.; Leroy, E.; Bresson, L.; Doris, E.; Loiseau, A.; Mioskowski, C. *J. Mater. Chem*. **2009**, *19*, 1271. (b) Pal, S.; Vivekchand, S. R. C.; Govindaraj, V.; Rao, C. N. R. *J. Mater. Chem*. **2007**, *17*, 450. (c) Zhi, C.; Bando, Y.; Wang, W.; Tang, C.; Kuwahara, H.; Golberg, D. *Chem.—Asian J*. **2007**, *2*, 1581. (d) Zhi, C.; Bando, Y.; Tang, C.; Golberg, D. *J. Am. Chem. Soc*. **2005**, *127*, 17144. (e) Wang, W.; Bando, Y.; Zhi, C.; Fu, W.; Wang, E.; Golberg, D. *J. Am. Chem. Soc*. **2008**, *130*, 8144. (f) Xie, S.-Y.; Wang, W.; Fernando, K. A. S.; Wang, X.; Lin, Y.; Sun, Y.-P. *Chem. Commun*. **2005**, 3670. (g) Zhi, C.; Bando, Y.; Tang, C.; Xie, R.; Sekiguchi, T.; Golberg, D. *J. Am. Chem. Soc*. **2005**, *127*, 15996.

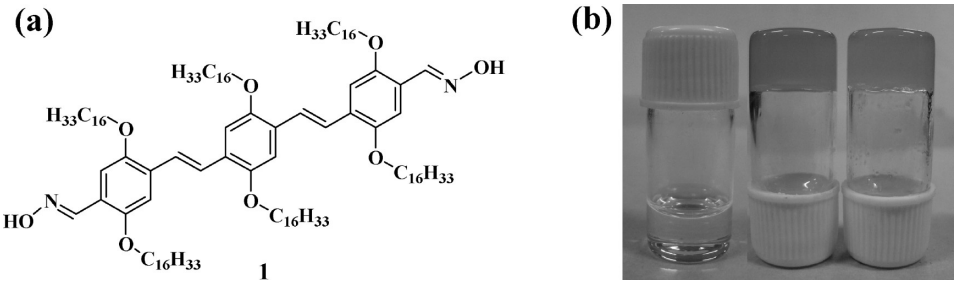

Figure 1. (a) Molecular structure of the gelator **1** used for the nanocomposite preparation with BNNTs. (b) Photographs showing (from left to right): gelator **1** in toluene as "sol", "gel", and BNNT-doped gel (nanocomposite).

In this context, organogels derived from low molecular weight gelators (LMWG)[8] hold a significant advantage to be excellent hosts for the preparation of various nanocomposites. The presence of self-assembled fibrillar networks in gels make them ideal for the dispersion of BNNTs due to their ability to interact mutually via various modes of noncovalent interactions.[9] Attractive van der Waals and π-stacking interactions among appropriate LMWG and BNNTs should lead to efficient wrapping and solubilization of the BNNTs in the chosen organic media. There are incentives for developing such nanocomposites as well. For example, one can bring about changes in the optical, mechanical, and thermal properties of the gel composites via the incorporation of even a small amount of BNNTs, and it may be possible to modulate the viscoelastic properties and thermal conductivity of the nanocomposites by the surface modification of BNNTs.

Although a number of gelators[10] have been designed for dispersing CNTs, to the best of our knowledge there has been no attempt to disperse BNNTs into a supramolecular gel matrix. The gelator that we have chosen here for this purpose is made up of an *all-trans* tri-(*p*-phenylenevinylene) bis(aldoxime) (TPV, **1**) which is capable of forming a physical gel in aromatic hydrocarbons such as toluene (Figure 1a).[11] A transparent solution of **1** (10 mg/mL) in toluene is obtained upon brief heating (a "sol"), which upon cooling to room temperature over ~20 min develops into an immobilized viscoelastic mass (a "gel") which does not flow under the influence of gravity (Figure 1b). The above step leading to spontaneous gelation is hastened when repeated in the presence of 0.2 mg (3.2 wt %) of BNNTs. The following features in the organogel of **1** make it particularly suitable for BNNT solubilization. These are (i) aromatic π-surfaces of extended conjugation in **1** that are capable of supporting stacking interactions with BNNT guests, (ii) six *n*-hexadecyl chains that promote van der Waals interactions among the gelator molecules or any guest molecule that is endowed appropriately (e.g., BNNTs functionalized with either aliphatic chains), and (iii) the presence of hydrogen-bonding donor and acceptor groups at the terminal functional groups holds the self-supporting TPV organogel network. In order to evaluate the interaction of **1** with different types of BNNTs in gels through $\pi-\pi$ stacking and van der Waals interactions, BNNTs functionalized with either aliphatic chains or aromatic moiety were employed. Herein we present the synthesis and characterization of various BNNT nanocomposites in organogels of **1** and evaluation of their different physical properties.

Experimental Section

Materials. All reagents, starting materials, and silica gel for TLC and column chromatography were obtained from the best known commercial sources and were used as such. Solvents were distilled and dried prior to their use. Gelator **1** has been synthesized following a previously reported procedure.[11] Syntheses and functionalization of various BNNTs and preparation of the gel−BNNT composites are discussed below.

Preparation of BN Nanotubes. An intimate mixture of finely ground MWCNTs (0.36 g) and H_3BO_3 (0.62 g) was taken in an 8 mm quartz tube closed at one end and held vertically inside a larger quartz tube placed in a tubular furnace. NH_3 gas was passed through the quartz tube (flow rate 10 sccm), and the temperature of the furnace, maintained initially at 200 °C for 2 h, was slowly raised to 1300 °C and maintained at that temperature for 3 h. Pure BNNTs were obtained as white deposits formed near the mouth of the quartz tubes and were characterized by SEM, TEM, and XRD studies as reported.[12]

Synthesis of BN−TBA, BN−TOA, and BN−TPP. For the preparation of BN−TBA and BN−TOA, 2 mL of TBA or TOA was added to 3 mg of BN nanotubes inside a round-bottom flask, respectively. The individual mixture was heated to 80 °C and kept at this temperature for 12 h and sonicated intermittently for 5−6 times (for ~5 min each time). For the preparation of BN-TPP, 1 g of TPP was mixed with 3 mg of BNNT and dispersed in 4 mL of toluene, and the resulting mixture was heated at 80 °C for 12 h with subsequent intermittent sonication. In each case, the resulting mixture was centrifuged and washed thoroughly with toluene in order to remove any unreacted starting materials (TBA, TOA, or TPP). The functionalized BNNTs were finally characterized using IR, ^{1}H NMR, ^{13}C NMR, TEM, SEM, and Raman spectroscopy to ascertain their purity.

Preparation of Gel−BNNTs Nanocomposites. A solution of the gelator, **1** in toluene was heated at a temperature of 60 °C. Into this solution specified amount of solid BNNT was added and then sonicated for ~1 min, and the resulting mixture was kept at room temperature for 20 min. Then the resulting mixture was converted into gel confirmed by "stable to inversion" method

(8) (a) Terech, P.; Weiss, R. G. *Chem. Rev.* **1997**, *97*, 3133–3160. (b) George, M.; Weiss, R. G. *Acc. Chem. Res.* **2006**, *39*, 489–497. (c) Weiss, R. G.; Terech, P. *Molecular Gels: Materials with Self-Assembled Fibrillar Networks*; Springer: Dordrecht, 2006. (d) Pal, A.; Ghosh, Y. K.; Bhattacharya, S. *Tetrahedron* **2007**, *63*, 7334. (e) Bhattacharya, S.; Pal, A. *J. Phys. Chem. B* **2008**, *112*, 4918. (f) Ragunathan, K. G.; Bhattacharya, S. *Chem. Phys. Lipids* **1995**, *77*, 13. (g) Bhattacharya, S.; Acharya, S. N. G.; Raju, A. R. *Chem. Commun.* **1996**, 2101. (h) Bhattacharya, S.; Acharya, S. N. G. *Chem. Mater.* **1999**, *11*, 3121. (i) Bhattacharya, S.; Krishnan-Ghosh, Y. *Chem. Commun.* **2001**, 185. (j) Bhattacharya, S.; Samanta, S. K. *Langmuir* **2009**, *25*, 8378.

(9) (a) Bhattacharya, S.; Srivastava, A.; Pal, A. *Angew. Chem., Int. Ed.* **2006**, *45*, 2934. (b) Basit, H.; Pal, A.; Sen, S.; Bhattacharya, S. *Chem.—Eur. J.* **2008**, *14*, 6534. (c) Pal, A.; Srivastava, A.; Bhattacharya, S. *Chem.—Eur. J.* **2009**, *15*, 9169. (d) Pal, A.; Basit, H.; Sen, S.; Bhattacharya, S. *J. Mater. Chem.* **2009**, *19*, 4325. (e) Srivastava, A.; Ghorai, S.; Bhattacharjya, A.; Bhattacharya, S. *J. Org. Chem.* **2005**, *70*, 6574.

(10) (a) Pal, A.; Chhikara, B. S.; Govindaraj, A.; Bhattacharya, S.; Rao, C. N. R. *J. Mater. Chem.* **2008**, *18*, 2593. (b) Srinivasan, S.; Babu, S. S.; Praveen, V. K.; Ajayaghosh, A. *Angew. Chem., Int. Ed.* **2008**, *47*, 5746. (c) Fujigaya, T.; Morimoto, T.; Niidome, Y.; Nakashima, N. *Adv. Mater.* **2008**, *20*, 3610. (d) Miyako, E.; Nagata, H.; Hirano, K.; Hirotsu, T. *Adv. Mater.* **2009**, *21*, 2819. (e) Xiao, F.; Liu, L.; Li, J.; Zeng, J.; Zeng, B. *Electroanalysis* **2008**, *20*, 2047. (f) Samanta, S. K.; Pal, A.; Bhattacharya, S.; Rao, C. N. R. *J. Mater. Chem.* **2010**, *20*, [J. Mater. Chem., DOI: 10.1039/C0JM00491J]. (g) Sivakkumar, S. R.; Kim, D.-W. *J. Electrochem. Soc.* **2007**, *154*, A134. (h) Rouse, J. H. *Langmuir* **2005**, *21*, 1055. (i) Liua, C.; Zhanga, J.; Hea, J.; Hub, G. *Polymer* **2003**, *44*, 7529. (j) Ferris, C. J., Panhuis, M. *Soft Matter* **2009**, *5*, 1466.

(11) Samanta, S. K.; Pal, A.; Bhattacharya, S. *Langmuir* **2009**, *25*, 8567.

(12) Deepak, F. L.; Vinod, C. P.; Mukhopadhyay, K.; Govindaraj, A.; Rao, C. N. R. *Chem. Phys. Lett.* **2002**, *353*, 345.

which showed no flow of the gelated mass under gravity. Diluted samples were examined individually using TEM, AFM, confocal, and FTIR spectroscopy studies. Composite "wet" and xerogels were examined further using SEM, rheology, DSC, and POM measurements. The thermal conductivity properties of the xerogel composites were also determined.

Transmission Electron Microscopy. Individual BNNTs were suspended in CCl_4 and drop-casted onto a carbon-coated copper grid (200 mesh size) and allowed to air-dry at room temperature, and TEM images were taken on a JEOL JEM 3010 operating with an accelerating voltage of 300 kV. Diluted toluene dispersion of each composite sample was drop-casted onto a carbon-coated copper grid (200 mesh size) and allowed to air-dry at room temperature. Then 10 μL of an aqueous 0.1% uranyl acetate solution was drop-coated on the sample placed on the grid and allowed to stand for 24 h and dried under vacuum. TEM images were taken at an accelerating voltage of 300 kV using a TECNAI F30 and JEOL JEM 3010.

Scanning Electron Microscopy. Individual BNNTs placed onto the brass stubs and analyzed on a FEI NOVA NANOSEM 600 machine operated at 15 kV. The composite samples were carefully scooped onto the brass stubs and were allowed to air-dry for overnight. The samples were then coated with gold vapor and analyzed on a Quanta 200 SEM operated at 15 kV.

Raman Spectroscopy. Individual solid BNNT samples were put under the laser, and Raman spectra of the BNNTs were recorded using a LabRAM HR high-resolution Jobin YvonHoriba HR800 Raman spectrometer using a He−Ne laser (λ = 632.8 nm).

Confocal Microscopy. A diluted toluene solution of **1** (2×10^{-4} M) containing 0.1 mg/mL BNNTs was drop-casted on a precleaned glass slide, and it was left overnight for drying in a dust-free environment and finally dried under vacuum. The confocal images were taken on a Leica TCS SP5 (Germany) microscope with an excitation wavelength of 488 nm.

FT-IR Spectroscopy. Diluted solution of **1** (1×10^{-3} M) in toluene incorporated with 9.95 wt % of different BNNTs were put onto the NaCl cell and dried and recorded on a Perkin-Elmer Spectrum BX machine.

NMR Spectroscopy. ^{1}H and ^{13}C NMR spectra of TBA−BN adducts were recorded on an AV 400 (Bruker) spectrometer using C_6D_6 as the solvent.[7b]

Differential Scanning Calorimetry. Gel samples in toluene were prepared, and their thermotropic behavior was investigated using a high-sensitivity differential scanning calorimetry using a CSC-4100 model multicell differential scanning calorimeter (Calorimetry Sciences Corp., Lindon, UT).

Samples were heated to sol and sonicated to make them homogeneous. An aliquot of each 0.4 mL clear sol sample was taken into DSC ampules. The ampules were sealed, and the samples were allowed to gelate upon gradual cooling to ambient temperature for overnight. The calorimetric measurement was carried out in the temperature range of 10−70 °C at a scan rate of 20 °C/h. At least two to three consecutive heating and cooling scans were performed. Baseline thermograms were obtained using same amount of the solvent in the respective DSC cells. The thermograms for the gel were obtained by subtracting the respective baseline thermogram from the sample thermogram using "CpCalc" software provided by the manufacturer.

Differential Scanning Calorimetry of Dried Composites. Dry composites were prepared by evaporating the solvents under ambient condition from the gel−BNNTs composites sample (10 mg/mL of **1** with 0.1 mg/mL BNNTs in toluene). The transition temperatures were determined using a differential scanning calorimeter (DSC; Perkin-Elmer, Model Pyris 1D) with heating and cooling rate fixed at 5 °C/min for all the measurements. This technique was used to detect the thermal transitions and to monitor the rate of flow from the sample during phase changes in the temperature change of 25−150 °C.

Polarized Optical Microscopy. 200 μL of sol (10 mg/mL of **1**) or nanocomposites (10 mg/mL of **1** doped with 0.1 mg/mL BNNTs) in toluene were placed on a glass slide and slowly allowed to be dry under ambient condition. Then it was covered with the coverslip, and the changes of textures of the sample were observed using polarized light microscope (Olympus BX51) provided with a heating stage (Mettler FP82HT) and a central processor (Mettler FP90). The heating and cooling rate was fixed at 10 °C/min for all the samples.

Rheological Studies. An Anton Paar 100 rheometer using a cone and plate geometry (CP 25-2) was utilized. The gap distance between the cone and the plate was fixed at 0.05 mm. The composite sample was scooped on the plate of the rheometer. Stress amplitude sweep experiment was performed at a constant oscillation frequency of 1 Hz for the strain range 0.001−550 at 20 °C. The rheometer has a built-in computer which converts the torque measurements into either G' (the storage modulus) and G'' (the loss modulus) in oscillatory shear experiments.

Thermal Conductivity. Thermal properties were characterized by thermal conductivity measurement in Thermal Transport Option (TTO) in a Physical Property Measurement System (PPMS, Quantum Design). Measurements were taken in four probe configuration, and contacts were made with gold-coated copper strips using silver-filled H20E epoxy (Epoxy Technologies).

Results and Discussion

Preparation and Characterization of Functionalized BNNTs. BNNTs were prepared via carbothermal reduction of a mixture of multiwalled carbon nanotubes (MWCNTs) and boric acid in the presence of ammonia at 1300 °C.[12] For achieving improved solubilization of BNNTs in solvents in which gelator **1** formed a physical gel, the BNNTs were functionalized via Lewis acid−base complexation between the electron-deficient BNNTs and electron-rich tertiary amines or phosphine bases.[7b] The advantage of this method is that it maintains the integrity and the aspect ratio of BNNTs and prevents defect formation during functionalization unlike in the covalent functionalization method adopted for CNTs where the CNT framework gets permanently damaged.[13] Various capped BNNTs were therefore synthesized by the functionalization of the BNNTs using triphenylphosphine (TPP), tributylamine (TBA), or trioctylamine (TOA) to furnish the resulting BNNT−TPP (BN−TPP), BNNT−TBA (BN−TBA), and BNNT−TOA (BN−TOA), respectively (see Experimental Section).

We examined the ^{1}H and ^{13}C NMR spectra of BN−TBA in comparison with the spectra of TBA alone. A small increase in the ^{1}H NMR chemical shift by ~0.02 ppm in the amine−BN adduct was observed. In the case of ^{13}C NMR spectra, significant increases in the chemical shifts of the γ and δ carbons by ~0.4 ppm and a decrease in the chemical shift of the β carbon atom by ~0.3 ppm were observed. The chemical shift of the α carbon was also found to be higher in the amine−BN adduct by ~0.1 ppm.

Transmission electron microscopy (TEM) images of the capped BNNTs confirm the tubular shape with high aspect ratio (Figure 2a−d). The outer diameter of the BNNTs was in the ~40−50 nm range and showed the multiwalled nature with a typical wall thickness of ~10 nm as revealed from the HRTEM images (Supporting Information, Figure S1). Upon capping the BNNTs with the individual amines or phosphine, the diameters increased to 60−80 nm. The results obtained from scanning electron microscopy (SEM) images were in accordance with the TEM results and confirmed the high aspect ratio of the nanotubes, with the diameters in the ~60−80 nm range for the capped

(13) (a) Banerjee, S.; Hemraj-Benny, T.; Wong, S. *Adv. Mater.* **2005**, *17*, 17. (b) Hirsch, A. *Angew. Chem., Int. Ed.* **2002**, *41*, 1853. (c) Aviles, F.; Cauich-Rodriguez, J. V.; Moo-Tah, L.; May-Pat, A.; Vargas-Coronado, R. *Carbon* **2009**, *47*, 2970.

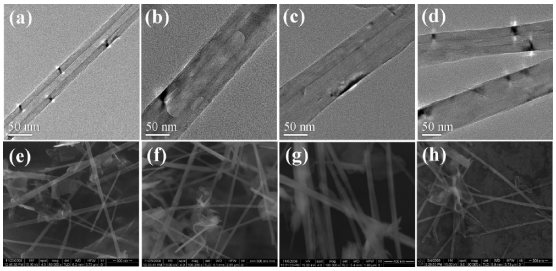

Figure 2. TEM and SEM images of (a, e) BN nanotube, (b, f) BN−TPP, (c, g) BN−TBA, and (d, h) BN−TOA.

BNNTs (Figure 2e−h). Raman spectra of both BNNTs and functionalized BNNTs showed the presence of characteristic 1365 cm^{-1} band due to the E_{2g} tangential mode (Supporting Information, Figure S2).[14]

Preparation and Characterization of Gel−BNNTs Nanocomposites. Formation of nanocomposites from the gelator **1** with the BNNTs is favored by the aromatic backbone of the latter, which makes it amenable to interaction with **1**. BN−TOA and BN−TBA possess long (C_8) and short (C_4) aliphatic chains, respectively, and these chains allow effective association with the aliphatic chains of the host gelator molecules. In case of BN−TPP, the aliphatic hydrocarbon chains are replaced by phenyl rings which interact through $\pi-\pi$ stacking with the π-surface of **1**. We prepared various organogel−BNNT composites by doping a small amount of BNNTs into the organogel matrix of **1** in toluene (Experimental Section). Confocal microscopy images of the composites showed red emission and the presence of three-dimensional (3D) bundles of fibers (diameter ~5−6 μm) when excited at 488 nm. Notably, in the nanocomposites containing BNNTs, the fibers showed more ordered structures with alignment in a directional fashion (Supporting Information, Figure S3). SEM images show the presence of fibrillar networks throughout the nanocomposite with a fiber diameter range of ~400−500 nm for the gel of **1** alone. Incorporation of BNNTs in the nanocomposite appears to induce collation of the fibers, leading to the formation of considerably thicker fibers. In the case of composites containing BN−TBA, BN−TOA, and BN−TPP, thicker fibers were formed presumably because the long aliphatic chains and aromatic rings on the BNNT surfaces are available for interactions intimately with the $-C_{16}H_{33}$ chains and the π-surface of the TPV backbone of **1**, respectively (Figure 3a−e). TEM images provide a clearer picture and corroborate the existence of molecular level interactions in the nanocomposites proposed here. Clear, "defect"-free tubes are observed in the TEM image of unfunctionalized BNNTs (Figure 3f). The TEM image of **1** exhibits a three-dimensional fibrous network formed by the entanglement of the self-assembled nanofibers of high aspect ratio and diameter of the fibers ranged from 50 to 150 nm (Figure 3g). Upon incorporation of BNNTs into the gel network, the fibers in the gel network further bundle to produce thicker fibers. Moreover, the wrapping of the gelator onto the BNNTs increases the diameter of the individual nanotubes by ~30−40 nm (Figure 3h−o). Magnified TEM images show nanotube-encapsulated TPV self-assembled structures, indicating the formation of fiber-reinforced supramolecular networks (Figure 3h,j,l,n). The interactions and the mode of self-assembly may be envisioned from a model generated by invoking the $\pi-\pi$ stacking, van der Waals, and the hydrogen-bonding interactions associated with them as shown in Figure 3p.

(14) Arenal, R.; Ferrari, A. C.; Reich, S.; Wirtz, L.; Mevellec, J. -Y.; Lefrant, S.; Rubio, A.; Loiseau, A. *Nano Lett.* **2006**, *6*, 1812.

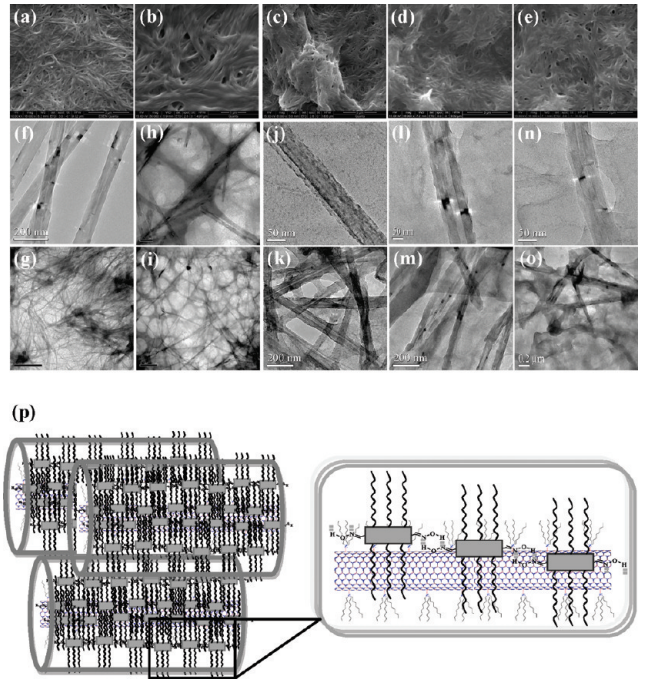

Figure 3. SEM images of dried gels of (a) **1**, (b) **1** + BN, (c) **1** + BN−TOA, (d) **1** + BN−TBA, and (e) **1** + BN−TPP. TEM images of (f) BN nanotubes, (g) nanofibers of **1**, (h, i) **1** + BN, (j, k) **1** + BN−TPP, (l, m) **1** + BN−TBA, and (n, o) **1** + BN−TOA. (p) Schematic representation of **1**−BNNT self-assembly formation.

FT-IR Spectroscopy. Evidence for the interaction of BNNTs with **1** is also obtained from the FTIR spectra of the composites.[15] The IR band at 1365 cm^{-1} is characteristic of B−N stretching in the BNNTs. The stretching frequency of the xerogel of **1** shows bands between 1100 and 1500 cm^{-1} for the asymmetric stretching and bending modes. When we compare the IR spectra of the composites with that of BNNTs and gelator, we notice decrease in the intensity of the 1100−1500 cm^{-1} bands. This again indicates the existence of interaction between the gelator and the BNNTs (Supporting Information, Figure S4).

Differential Scanning Calorimetry (DSC). In order to investigate the thermal behavior of the gel nanocomposites, DSC experiments were performed with the toluene gel of **1** and its composites with various BNNTs in toluene. An increase in the sol-to-gel transition temperature (T_f) for the nanocomposites containing small amount of BNNTs (1.96 wt %) was observed although the gel-to-sol transition temperatures did not show any significant changes (Figure 4a).[16] The extent of increase in the phase transition temperature was found to depend on the nature of interactions between the TPV backbone in **1** and the BNNTs. The T_f for the gel of **1** (10 mg/mL) was 25.7 °C, whereas in the case of **1** + BN and **1** + BN−TPP, where mainly $\pi-\pi$ interactions prevail, the T_f values increased to 26.3 and 26.6 °C, respectively. However, for BN−TBA and BN−TOA, where additional van der Waals interactions are feasible through long chains, the T_f increased to 26.8 °C.

The dried gel and the corresponding BNNTs composites were also investigated using DSC. When the xerogel of **1** alone was cooled from the molten state, peaks emerged at 113.3 and 123.1 °C (Figure 4b). However, when the xerogel of nanocomposites were

(15) (a) Zhi, C.; Zhang, L.; Bando, Y.; Terao, T.; Tang, C.; Kuwahara, H.; Golberg, D. *J. Phys. Chem. C* **2008**, *112*, 17592. (b) Ravichandran, J.; Manoj, A. G.; Liu, J.; Manna, I.; Carroll, D. L. *Nanotechnology* **2008**, *19*, 085712.

(16) Zhi, C.; Bando, Y.; Wang, W.; Tang, C.; Kuwahara, H.; Golberg, D. *J. Phys. Chem. C* **2007**, *111*, 18545.

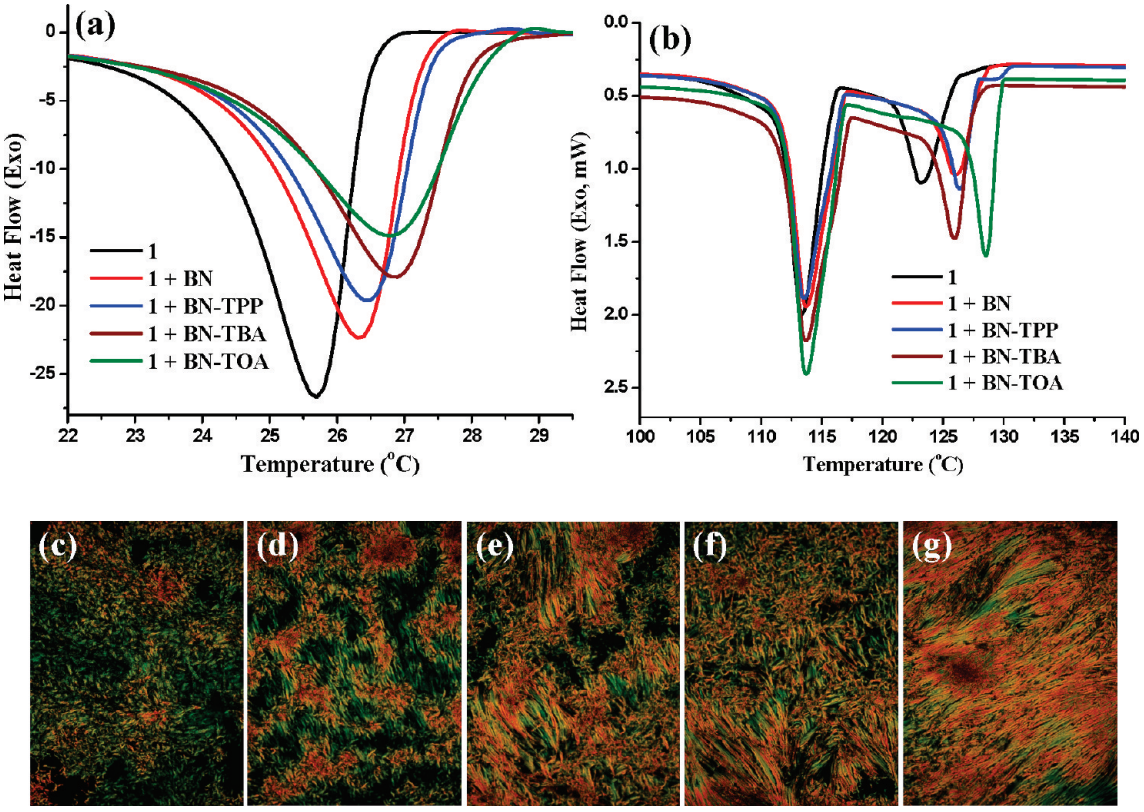

Figure 4. DSC of (a) the toluene gel and (b) the xerogel of **1** and **1**−BNNTs composites ([**1**] = 10 mg/mL). POM images of dried composites of (c) **1**, (d) **1** + BN, (e) **1** + BN−TPP, (f) **1** + BN−TBA, and (g) **1** + BN−TOA (1.96 wt % of BNNT was used with respect to **1** in each case).

cooled from the molten state, the solidification temperature (T_s) increased upon incorporation of 1.96 wt % BNNTs. For the composite xerogels, two peaks were observed in all instances in the cooling cycle at 113.6 and 126.1 °C for **1**−BN, 113.5 and 126.4 °C for **1**−BN−TPP, 113.7 and 126.0 °C for **1**−BN−TBA, and 113.7 and 128.5 °C for **1**−BN−TOA. Such rise in the T_s suggests a change in the organization of the composite compared to the one in gel alone which brings about more "order" in the nanocomposites.

Polarized Optical Microscopy (POM). The above results from DSC measurements on the xerogel of **1** and the corresponding composites prompted us to find out their texture under a polarized optical microscope. Under polarized light, the xerogel of **1** showed presence of birefringent three-dimensional (3D) textures upon cooling from the isotropic melt (Figure 4c), indicating an anisotropic growth of the 3D aggregates by the gelator molecules.[10b,17] The anisotropic growth of the TPV molecules were monitored by taking snapshots at progressively decreasing temperatures from the isotropic melt which showed different birefringent textures for the nanocomposites compared to that of the xerogel (Supporting Information, Figure S5). When the dried nanocomposites with different BNNTs (1.96 wt % with respect to **1**) were examined under the polarized light, they showed different types of 3D birefringent textures, indicating directional character and compactness in the self-assembly of **1** leading to the formation of more "ordered" structures (Figure 4d−g). Since the alkyl chains in BN−TBA and BN−TOA and the aromatic rings in BN−TPP interact with the long chains and π-surface of **1**, therefore an alignment in the anisotropic growth of the gelator molecules can take place. The effect of doping a small amount of BNNTs is thus sufficient to modify the order and the textures (organization) of the composites.

Rheological Studies. To probe the influence of BNNT incorporation on the viscoelasticity and the flow behavior of gel, rheological studies were performed. Frequency sweep measurements of gel of **1** and the composites containing 0.83 wt % of BNNT (with respect to **1**) furnish the storage modulus (G') and loss modulus (G'') as a function of angular frequency (ω) (Figure 5a). The G' and G'' show a plateau region over the entire angular frequency range (0.1−100 rad/s) at 0.01% strain amplitude. A 20-fold higher G' value over G'' suggests a substantial elastic response of the gels. The G' of the composite is ∼3 times more than that of the gel, and hence the composite gel is more viscoelastic than that of the gel alone. A gradual and monotonous increase in the G' was seen with the increased loading of the BNNTs in the nanocomposite, resulting in progressively more viscoelastic properties of the composites (Supporting Information, Figure S6).

In a typical oscillatory sweep experiment, the stress vs strain plot yields the complex modulus (G^*) which is composed of two components: (i) G', representing the ability of the deformed material to restore its original geometry, and (ii) G'', representing the tendency of a material to flow under stress. For materials like gels, G' is an order of magnitude greater than G'', showing the dominant elastic behavior of the system, i.e., resistance to flow under applied stress. An applied stress above which the gel starts to flow is called the yield stress (σ_y), and this refers to a particular stress at which G'' becomes greater than G' for a gel where the property changes from a dominant elastic-solid-like behavior to a dominant viscous-liquid-like behavior.[18] The gel alone here

(17) Kumar, S.; Bisoyi, H. K. *Angew. Chem., Int. Ed.* **2007**, *46*, 1501.

(18) (a) Bychuk, O.; Shaughnessy, B. O. *Phys. Rev. Lett.* **1995**, *74*, 1795. (b) Menger, F. M.; Caran, K. L. *J. Am. Chem. Soc.* **2000**, *122*, 11679. (c) Terech, P.; Pasquier, D.; Bordas, V.; Rossat, C. *Langmuir* **2000**, *16*, 4485.

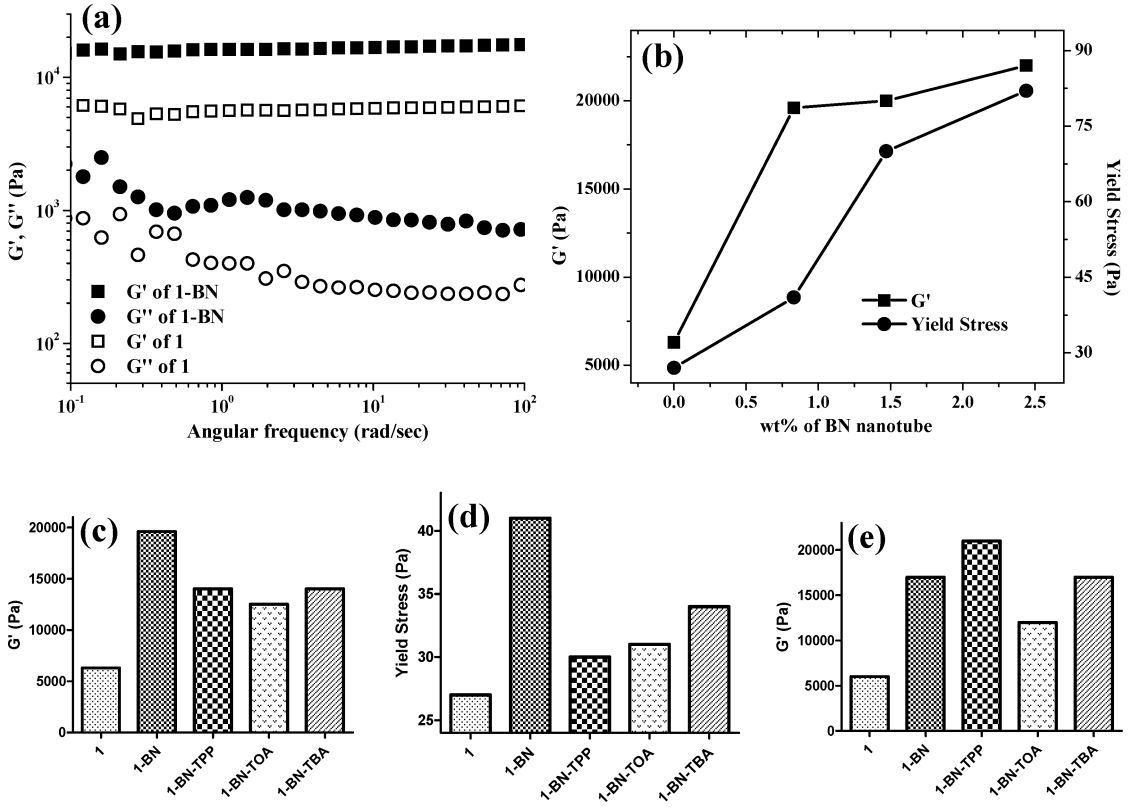

Figure 5. Plot of (a) storage (G') and loss modulus (G'') of **1** and the nanocomposite gel (0.83 wt % of each BN nanotubes) as a function of angular frequency at 0.01% strain amplitude; (b) typical amplitude sweep experiment showed G' and yield stress (σ_y) with concentration variation of BNNTs in nanocomposite gel of **1**. Comparison of (c) G' and (d) yield stress (σ_y) of **1**−BNNTs composites in a amplitude sweep experiment, (e) comparison of G' of **1**−BNNTs composite gels with different types of functionalized BNNTs in toluene in a frequency sweep experiment (strain amplitude = 0.01%) ([**1**] = 10 mg/mL in all cases).

exhibited a viscoelastic storage modulus of ∼6300 Pa, and it began to flow at an applied stress (σ_y) of ∼27 Pa (Figure 5b). Incorporation of a small amount (0.83 wt %) of BNNT rendered the gels significantly rigid ($G' \approx 19\,600$ Pa), and it started to flow only under a considerably higher applied stress ($\sigma_y \approx 41$ Pa). The solidlike behavior (G') of the composites increases with the increase in the amount of BNNTs in the composite, and the corresponding composites started to flow under increasingly higher applied stress (σ_y).

Enhanced viscoelastic-solid-like behavior was observed for each of the nanocomposites with the functionalized BNNTs compared to the gel alone as in each case the G' value was greater than that of the gel (Figure 5c). The corresponding yield stress (σ_y) required for dominating viscous-liquid-like behavior of the gel also increased for the composites (Figure 5d). A bar diagram in Figure 5e shows increased storage modulus (G') for the different **1**−BNNTs nanocomposites (containing 0.83 wt % of BNNTs) spanning the entire angular frequency range at 0.01% strain amplitude compared to that of **1**. This again indicates higher viscoelasticity of the composites upon incorporation of BNNTs.

A possible interaction of these functionalized BNNTs with the gelator may occur through either of the two ways: (i) via $\pi-\pi$ interaction between the π-conjugated aromatic backbone of the gelator with the π-surfaces of the BN nanotubes or the phenyl ring of the attached triphenylphosphine functionalized caps or through (ii) van der Waals interactions between the *n*-hexadecyl chains of the gelator with the dangling aliphatic chains of the functionalized BNNTs. There may be a competition between these two modes of interactions which defines the viscoelasticity of the nanocomposite in the gel state. In case of the functionalized BNNTs, both the π-stacking and the van der Waals interactions may allow association with the gelators. However, since the functionalized BNNT surfaces are modified by the alkyl/aryl chains, the π-stacking could be relatively reduced and the rigidity/compactness of the resulting BNNT−gel assembly may be achieved significantly by van der Waals interactions. Hence, the increase in the storage modulus for the functionalized BNNT−gel mixture was found to be less compared to that of the nonfunctionalized BNNT−gel composites. With BNNTs bearing longer aliphatic chain (in case of TOA), the reduction in the π-stacking should be more pronounced than that with a shorter alkyl chain (for TBA). Thus, a lesser storage modulus for the composites doped with BNNTs having longer alkyl chains (TOA) is manifested. In the case of BN−TPP, the propensity of π-stacking interaction was further improved by the peripheral TPP moiety, and hence increased G' was observed with its composites in gel compared to composites containing either BN−TBA or BN−TOA.

Thermal Conductivity Studies. The thermal conductivity of a film of gel of **1** and **1**−BNNT nanocomposite (having 10 wt % of BNNTs with respect to **1**) was measured as a function of temperature. The composite showed an improved thermal conductivity compared to **1** for the entire region of temperature (Figure 6a). A bar diagram shows an increase in the thermal conductivity value for the nanocomposites at various temperatures, demonstrating 134% increase at 0 °C, 126% increase at 30 °C, and 116% increase at 60 °C (Figure 6b). These increments compare well with those of the reported polymer−BNNT composites.[19] The composite is reinforced by the π-stacking interactions between **1** and the BNNTs. As the BNNTs alone

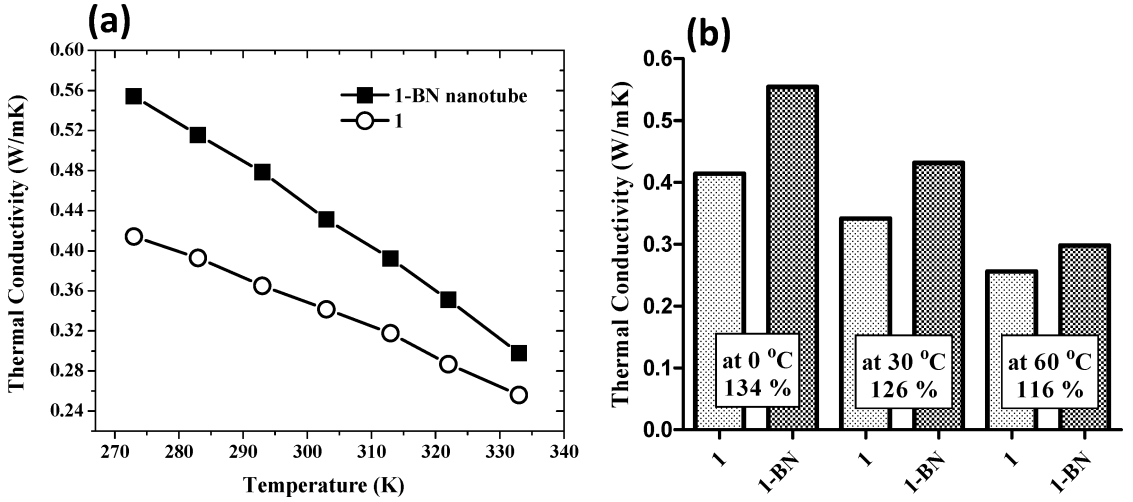

Figure 6. (a) Thermal conductivity of the xerogel of **1** and **1**−BNNT composite films (10 wt % BNNT with respect to **1**) as a function of temperature. (b) Bar diagram showing the % increment in the thermal conductivity (W/mK) at various temperatures of 0, 30, and 60 °C.

are known to be excellent thermal conductors,[20] so the composite shows higher thermal conducting property compared to that of the gelator alone.

Conclusion

In this work, we have successfully prepared and characterized new gel nanocomposites from a low molecular weight gelator based on the tri-(*p*-phenylenevinylene) system **1** and different types of BNNTs in toluene. Changes in the organization of the gel nanocomposites relative to the gel alone are readily seen from SEM images which show collation of gel fibers in a directional fashion to form thicker fibers in the composites. TEM images reveal wrapping of the gelator molecules around the BNNTs as evidenced from increase in the diameter of the BNNTs. Gelator−BNNT interactions in the composites are evident from the results obtained from the thermotropic studies. The sol-to-gel transition temperature of the gel increases upon incorporation of a small amount of each BNNT. Also, the solidification temperature increases for the xerogel of gel−BNNTs nanocomposites. Incorporation of BNNTs also alters the birefringent textures of the materials as evident from polarized optical microscopy. The reinforced aggregation of gelators on doping with BNNTs is further reflected from the mechanical properties of the nanocomposites. Rheological properties of the composites demonstrate the formation of rigid and viscoelastic solid-like assembly on BNNT incorporation. Furthermore, considerable increase in the thermal conductivity occurs in the composites compared to that in **1**. We have, thus, been able to define a relation between bulk properties of the composite with the molecular level features of doped BNNTs which enable convenient modulation of the properties upon external doping. Such soft BNNT composites should be useful in applications involving the design of thermally conducing coating materials.

Acknowledgment. We thank DST (J. C. Bose Fellowship to SB) and FMC, India for financial support, INI, and RRI for various Instrumental Facilities. S. K. Samanta is grateful to CSIR for a Senior Research Fellowship.

Supporting Information Available: Figure S1 showing HRTEM of the multiwalled BNNT, Figure S2 depicting Raman spectra of different types of BNNTs, Figure S3 showing confocal microscopy images of the dried gel−BNNTs composites, Figure S4 depicting FT-IR spectroscopy of the composites, Figure S5 showing POM images, and Figure S6 showing comparison of storage modulus (G') of the gel nanocomposites with varying weight of BNNTs in toluene. This material is available free of charge via the Internet at http://pubs.acs.org.

(19) (a) Terao, T.; Bando, Y.; Mitome, M.; Zhi, C.; Tang, C.; Golberg, D. *J. Phys. Chem. C* **2009**, *113*, 13605. (b) Zhi, C. Y.; Bando, Y.; Wang, W. L.; Tang, C. C.; Kuwahara, H.; Golberg, D. *J. Nanomater.* **2008**, Article ID 642036, DOI: 10.1155/2008/642036.

(20) Tang, C.; Bando, Y.; Liu, C.; Fan, S.; Zhang, J.; Ding, X.; Golberg, D. *J. Phys. Chem. B* **2006**, *110*, 10354.